

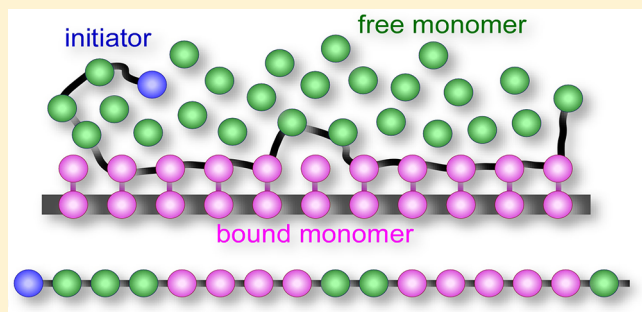
Computer Simulation of Template Polymerization Using a Controlled Reaction Scheme

Preeta Datta and Jan Genzer*

Department of Chemical & Biomolecular Engineering, North Carolina State University, Raleigh, North Carolina 27695-7905, United States

 Supporting Information

ABSTRACT: We employ a Monte Carlo simulation scheme based on the bond fluctuation model to simulate template polymerization via controlled polymerization scheme involving copolymerization of free monomers (A) and monomers bound to a template (B) that consists of linear or ring-like substrates with equidistant sites occupied by bound B monomers. Both A and B are chemically identical; i.e., there is no interaction potential acting between A and B. A new macromolecule is initiated in bulk by activation of an initiator; any monomer that is within the reaction distance (nearest neighbors) of the initiator can be incorporated into the chain. As the macromolecule grows, it adds either bulk (i.e., A) or template-bound monomers (i.e., B) to its chain. The living nature of the polymers is assured by eliminating any termination or chain transfer. We analyze the effect of the number and spacing of the B bound monomers on the substrate on the chemical composition and monomer distribution in the resultant A–B random copolymer. Our results reveal that the likelihood of B being incorporated in the A–B copolymer increases with increasing the number and density of the B monomers on the template substrate; the maximum sequence length of “polymerized” bound B monomers increases with increasing the number of bound B monomers present in a single substrate. Long consecutive sequences of B bound monomers in the A–B copolymer are formed when the B bound monomers are immobilized in space in high densities.



INTRODUCTION

The increasingly demanding industrial applications and the emerging uses of synthetic polymers require synthesis of specialty macromolecules. Synthetic homopolymers often lack perfect molecular-level definition; i.e., they possess nonuniform molecular weight distribution or distribution in tacticities. In addition, synthetic copolymers often exhibit chemical non-uniformity and randomness in the sequence of different types of units along the chains. This lack of definition arises from a number of causes, the most important ones being the statistical nature of the polymerization process and the absence of specificity in chain propagation. In many biological reactions, such as DNA replication or polypeptide synthesis, low molecular weight substrates and polymeric products are present in the reaction medium together with the macromolecular compounds, called matrices or templates, which control the synthetic process. The discovery of DNA replication, an elaborate template synthesis, has inspired the development of template polymerization.^{1,2} Polymer chemists have studied the effects of templates on various types of polymerization methods, including, chain- and step-growth during homo- or copolymerization. The most notable examples are the use of DNA-templated synthesis (DTS) and nucleic acid template synthesis to either elongate DNA and oligo-nucleotide strands or polymerize daughter monomers from a predefined DNA

sequence.³ While DTS is an attractive platform for the production of monodisperse polymers with well-defined chemical sequences, it has so far been limited primarily to biopolymers.

Template polymerization (also called molecular imprinting) is a process, which utilizes specific interactions between a preformed macromolecule (i.e., template) and a growing chain.^{1–5} It is characterized by geometrically predetermined paths of chain propagation. Template polymerization comprises three steps: (1) template–monomer complexation to form a linear array of monomers, (2) polymerization of bound monomers, and (3) separation of the daughter macromolecule from the mother template. The monomer units can bind to the template via various physical interactions, such as, hydrogen bonding, dipole–dipole or electrostatic forces, or by chemical bonding, such as disulfide bridging. In order to study template systems, one needs to compare the template process and products of the reaction with conventional bulk polymerization carried out under identical conditions, typically replacing the template by a low molecular nonpolymerizable entity. The effects of the template on the polymerization process and the

Received: December 18, 2012

Revised: February 24, 2013

Published: March 5, 2013

product are usually called “template effect” or “chain effect”.¹ The template effects can be classified as follows:^{1,2,4–6} (1) the kinetic effect (i.e., increased the reaction rate, change in kinetic equation), (2) the molecular effect (i.e., influence on the molecular weight and molecular weight distribution; ideally, the degree of polymerization of the daughter polymer is the same as the degree of polymerization of the template used, so-called replication), (3) the effect on tacticity (i.e., the daughter polymer can have a structure complementary to the structure of the template used), and (4) the effect on the sequence distribution of units (in case of template copolymerization). In this work, we explore the effect of templation on the average molecular weight, composition and sequence length distribution of the daughter polymers.

Advances in template polymerization can lead to better control of polymer properties. A few examples of influencing polymer properties, namely tacticity and chain organization, through templation have been reported in literature.^{7–9} Other potential applications include synthesis of ladder-like polymers, or surface-based template polymerizations for the production of intertwined structures, free-standing two-dimensional polymers and molecular sensors.^{9–12} The major applications of template polymerization are in the fields of analytical and biochemistry, medicine, pharmaceutical science, and catalysis. Molecularly imprinted polymers find application in separation techniques such as chromatography, electrophoresis, extraction and selective absorption of low-molecular weight compounds.^{13–16} Nanoreactors, separation membranes or catalytic carriers, can be fabricated by polymerizing monomer units attached to surfactant aggregates (i.e., templates) such as micelles, membranes and vesicles, or various nanostructures of one, two or three dimensions.^{17–20} In order to potentially harness Nature’s templation strategies to produce polymers with controlled lengths, tacticities, and sequences, we need to understand the factors that can affect template polymerization of simpler moieties. Experimental studies are often tedious and expensive because of the difficulties in separating the daughter polymer from the template. To this end, the vast parameter space can be explored easily and effectively with computer simulations.

In this work, we employ a Monte Carlo simulation scheme based on the bond fluctuation model²³ to simulate template polymerization via controlled polymerization scheme, involving copolymerization of free monomers (A) and monomers bound to a template (B) that consists of linear/ring-like substrates with equidistant sites occupied by bound monomers (B). Such a system can be realized experimentally by adsorbing monomer to liquid/solid, liquid/liquid, or air/liquid interfaces via physical or chemical interactions²¹ and then inducing polymerization by exposing these monomer-containing substrates to monomer/initiator mixtures. The main purpose of this work is to set up a framework that would facilitate understanding of the structure of the resulting copolymers under different system conditions. Gaining detailed insight into the structure of the copolymers grown via template polymerization will help comprehend how the properties of the daughter polymers depend on the densities of free monomers and initiators and the concentration and spacing of the bound monomers on the template as well as the template spatial arrangement. To accomplish this goal, we vary systematically the number of free monomers, the number of initiators, the number monomers bound to the template, the spacing between adjacent monomer units bound to the template, template spatial arrangement (i.e., shape, orientation)

and degree of flexibility of the substrate-bound monomers on the template. Upon testing the different parameters, we seek to identify how the aforementioned parameters affect the chemical composition and comonomer distribution in the resulting copolymers.

Different applications require that polymers be prepared on substrates comprising various geometries and dimensionalities, such as nanowires, Si/Au surfaces, porous materials or polymers with a stiff backbone. Depending on the geometry and the dimensionality of the substrate, the growing copolymer chains experience a diverse degree of confinement. For planar substrates (Si/Au wafers)²¹ or nanoporous substrates²² (i.e., zeolites), the added dimensionality can impose stronger spatial restrictions on the growing polymer chains as compared to rod-like substrates (i.e., nanowires, polymer backbones). In literature, there are some computational models for simulating the process of template polymerization^{26–29} where one of the polymerizing species (“sticky” units) is preferentially adsorbed onto a planar template or has a greater affinity for the planar template. However, those studies involve flat two-dimensional substrates, where the copolymer chains are much more restricted than in case of one-dimensional substrates. In this paper, we deal specifically with one-dimensional substrates because this is perhaps the simplest geometry to model and understand as it imposes the least spatial restriction on the growing copolymer chains.

For this work, we assume that the substrates are fixed in space with a monomer layer bound to it. In experiments, this corresponds to the case when Au–thiol chemisorption²¹ or organosilane chemistry is utilized to create a relatively stable self-assembled monolayer of bound monomers (e.g., acrylate functional groups attached to silane/thiol). A potential way to achieve one-dimensional rigid templates with covalently bound monomeric units is to synthesize a polycarbodiimide backbone with specific side-chain monomeric functionalities (such as methacrylate/acrylate).³⁰ The density of the bound monomers on the substrate is the key parameter in template polymerization. Depending on the grafting density, templation might be favored due to proximity of monomer units or hindered due to steric effects. Substrate shape can potentially impose confinement effects on the growing copolymer chains. We explore two cases of substrate curvatures, i.e., rod-like substrates and ring-like substrates. With the present setup, extension to flat, concave or convex two-dimensional substrates is straightforward.

SIMULATION MODEL

We use a Monte Carlo (MC) simulation scheme to model the “living”/controlled radical polymerization (CRP) based on the bond fluctuation model (BFM) in the *NVT* ensemble.²³ The substrates, monomers, and polymers reside on a three-dimensional cubic lattice. All possible permutations and sign inversions of the following vector families represent the allowed set of moves: $P(2,0,0) \cup P(2,1,0) \cup P(2,1,1) \cup P(2,2,1) \cup P(3,0,0) \cup P(3,1,0)$. This prevents any bond from crossing and polymers from overlapping. In this implementation, each bead on the lattice represents an effective monomer unit. The simulation results reported here have been carried out on a cubic lattice $50 \times 50 \times 50$, with periodic boundary conditions applied in all directions. Because each monomer corresponds to eight sites effectively, the full lattice occupancy is achieved at 15 625 sites. The computer simulations follow the general scheme of individual steps reported in an earlier work by one of

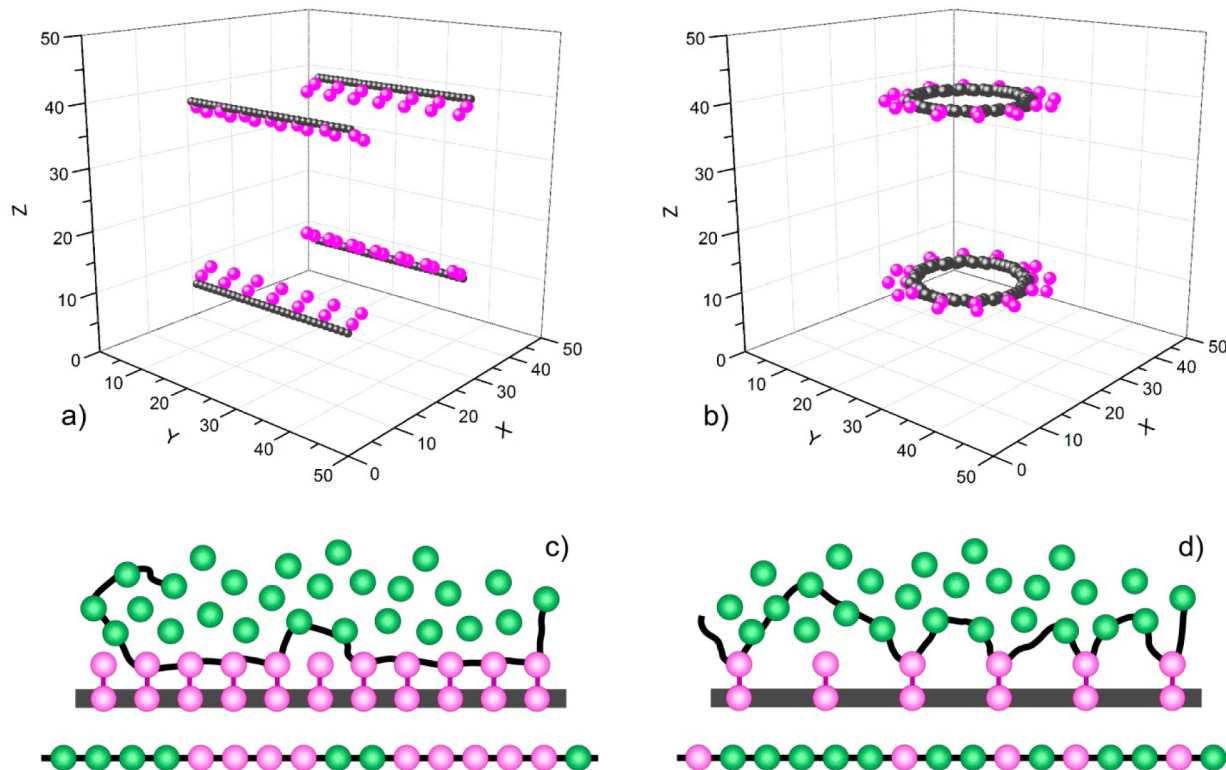


Figure 1. (a) Rod-like substrates (black) with grafted bound monomers (magenta), (b) Ring-like substrates (black) with grafted monomers (magenta), (c) copolymers formed by combination of free monomers (green) and bound monomers (magenta)—high grafting density of monomers, (d) copolymers with bound “unimers”—low grafting density of monomers on substrate.

the authors.²⁴ The values of the parameters intrinsic to the MC simulation scheme are held constant during all the runs, namely reaction probabilities for initiators and living radicals are both 1 and the probability of reaction vs motion is 0.01. A low value of the reaction probability assures controlled polymer growth. For details of the model and the choice of parameters see refs 24 and 25.

In our computer simulations, the B monomers are bound to either rod-like or ring-like substrates, whose position is fixed in space (cf. Figure 1). The rod-like substrates are four in number and are positioned symmetrically in the cubic lattice, with either 7 or 16 bound B monomers grafted on each of the substrates. Thus, the total number of bound monomers ([B]) is either 28 or 64. The grafting density of the bound monomers on the substrates (σ_B) is, defined as the ratio of the number of bound monomers that are present on a substrate relative to the maximum number of monomers that can be accommodated on that substrate. For ring-like substrates, we have 24 or 48 B bound monomers equally distributed between two rings placed symmetrically in the cubic lattice (cf. Figure 1). The bound monomers can be oriented in four different ways relative to the ring-like substrate: in-plane, 30° incline, 60° incline or normal (*vide infra*). Figure 1 shows only the in-plane orientation of bound monomers on a ring. We refer back to the different orientations briefly in a later section (cf. Figure 10). The B bound monomers are attached to the substrates by either rigid or flexible bonds. For most of the simulations, we keep the B monomers bound rigidly in space. We later introduce flexibility in the bound monomers such that the bond between the substrate and the bound monomer can stretch and rotate in accordance with the BFM formalism. In addition to the bound B monomers, there are free A monomers present in bulk.

Although both A and B are identical, i.e., there is no interaction potential acting between A and B, we use this nomenclature to distinguish between the polymers formed of free monomeric units only and those formed of both bound and free monomeric units. In addition, there are free initiators present in bulk. The numbers of A monomers and initiators are denoted as [A] and [I], respectively. Two different types of polymers can form during the simulation: homopolymers comprising only A units (i.e., A homopolymers) and copolymers containing both A and B units (i.e., A–B copolymers). Figure 1 shows schematically that the “degree of randomness” in the A–B copolymer depends on the spatial distribution of the B units on the template. To this end, B units spaced closely on the template form random-blocky copolymers (i.e., having longer consecutive sequences of B) while sparsely distributed B monomers result in “truly random” copolymers (i.e., having discretely and randomly spaced B units).

Our system is “truly living”, i.e., the chains do not undergo termination of chain transfer.²⁵ The implicit solvent model (no explicit solvent molecules are included in the simulations) is presumed to be valid for modeling the growth of “living” chains under good solvent conditions.²⁵ The initiator molecules and free monomers are initially distributed homogeneously throughout the lattice. In our simulations, the initial number of free monomers ([A]) is set to be either 3125 or 6250, which corresponds to the lattice occupancy of 20% or 40%, respectively. The initial number of initiators ([I]) is chosen to be either 12 or 125, giving rise to a maximum number of polymers equal to 12 or 125, respectively, that can exist for a given simulation. After placing the monomers and initiators on the lattice, we perform an initial equilibration run for 10^9

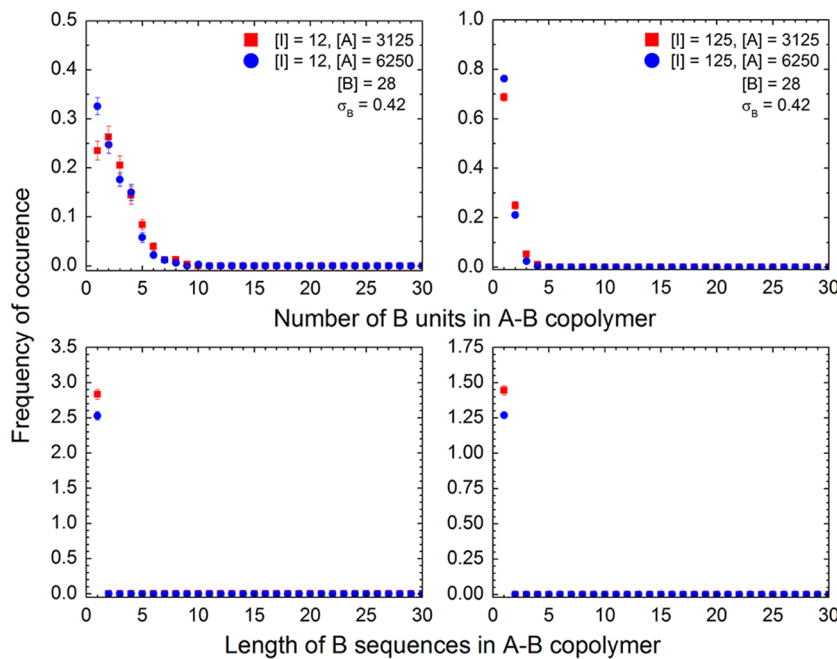


Figure 2. Comparison of the number and sequence length distributions of B bound monomers in A–B copolymers, averaged over 10 simulation runs, for different number of initiators ($[I] = 12$ and 125) and free monomers ($[A] = 3125$ and 6250) for rod-like substrates.

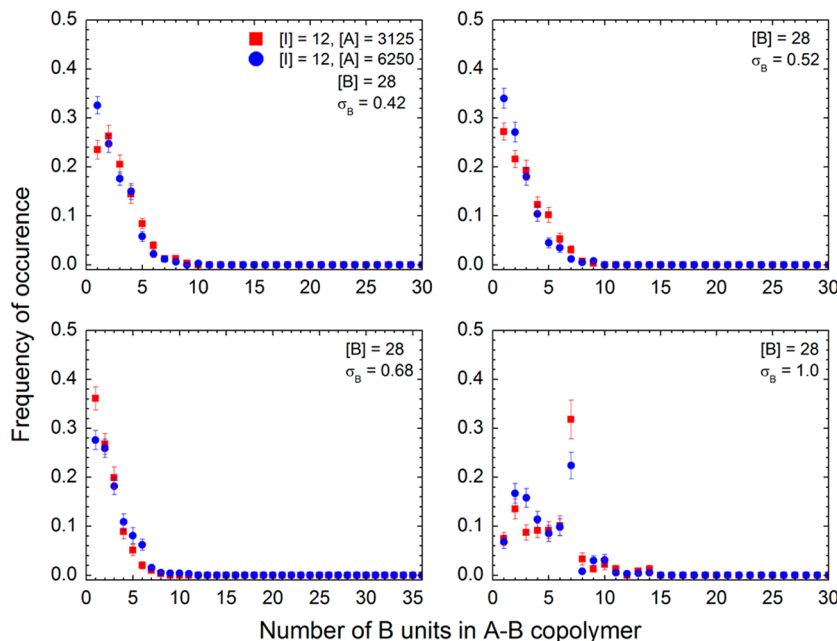


Figure 3. Comparison of the number distribution of B in A–B copolymers, averaged over 50 simulation runs, for different grafting densities on rod-like substrates (σ_B).

Monte Carlo steps (MCS) per bead to obtain a randomly distributed configuration. We use the equilibrated configuration as the input for the MC simulation. The reactive MC algorithm commences after a secondary short equilibration run ($\approx 10^5$) and runs for a predetermined number of MCS, typically 10^9 , in order to achieve the same conversion.

Chain statistics (i.e., molecular weight, polydispersity index) and the coordinates of the monomers of each polymer and all monomers are stored periodically after several thousand MCS. In order to obtain good statistics, we perform 50 MC simulations runs for every set of input parameters. In order to understand the effect of different parameters (i.e., $[B]$, σ_B ,

$[A]$, $[I]$, substrate shape, bound monomer orientation and flexibility), we monitor the number distribution of bound B monomers and the sequence length distribution in the A–B copolymers, normalized by the number of copolymers formed. While the number distribution gives us a quantitative estimate of the incorporation of bound B monomers in A–B copolymers, the sequence length distribution offers a qualitative insight into the comonomer distribution in the A–B copolymers. In addition, we also report the number of A–B copolymers and the mole fraction of bound B monomers present in the A–B copolymers.

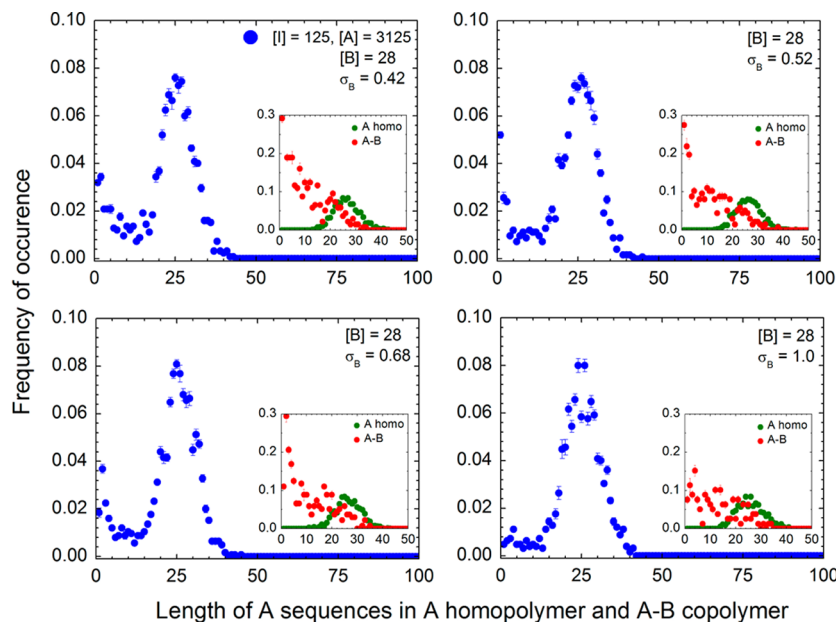


Figure 4. Sequence length distribution of free A monomers in polymer chains corresponding to different grafting densities of the template. The insets: Sequence length distribution of A units in copolymers and homopolymers for different grafting densities on rod-like substrates (σ_B). The latter data are normalized by the number of chains.

RESULTS AND DISCUSSION

To facilitate the discussion, we set $[B] = 28$, and $\sigma_B = 0.42$. We will explore the effect of these two parameters later in the paper. In Figure 2, we plot the normalized number distribution of bound monomers $[B]$ in the A–B copolymers (upper row) and the corresponding distribution of the sequence lengths, normalized by number of copolymers (lower row) for two concentrations of free monomers ($[A]$) equal to 3125 (red squares) and 6250 (blue circles) and two free initiator concentrations ($[I]$) equal to 12 (left column) and 125 (right column). The data in Figure 2 reveal that the probability of incorporating the B monomers into the A–B copolymer is not affected by the number of free A monomers. Altering the concentration of free initiators does have an effect on the likelihood of finding the B monomers inside the A–B copolymer. A more than 10-fold increase in $[I]$ (from 12 to 125) reduces the maximum number of B monomers per copolymer from ≈ 8 to ≈ 4 while concurrently increasing the occurrence of A–B copolymers that have only a single B bound monomer. Because of an increased $[I]$ more polymer chains are generated in the system, which reduces the number of B bound monomers available per growing chain. Thus, by increasing $[I]$, it is more likely to form more A–B copolymers but less likely for a growing A–B chain to incorporate many bound B monomers. We will refer back to the effect of the number of initiators on the polymerization process later in this section.

We now set $[I] = 12$ and $[B] = 28$ and increase σ_B from 0.42 to 1.0. The normalized number distributions of bound B monomers per A–B copolymer chain for the different values of σ_B are plotted in Figure 3. The maximum number of B monomers per copolymer increases with increasing σ_B irrespective of the number of free monomers ($[A]$). This effect becomes most prominent at the highest grafting ($\sigma_B = 1$); the maximum number of B per copolymer increases from ≈ 7 (for $\sigma_B < 1$) to ≈ 13 (for $\sigma_B = 1$). Note that for $\sigma_B = 1$ there is a distinct peak corresponding to 7 bound B monomers per A–B copolymer indicating that all of the 7 bound B monomers in

each substrate (recall that given $[B] = 28$ and 4 identical substrates bearing the bound B monomers, there are 7 monomers per substrate) can be potentially incorporated in a single chain at the highest grafting density. This implies that we can grow polymer chains that mimic perfectly the template when the B monomeric units are spaced as close as possible along the template. We attribute this behavior to the “proximity effect”; i.e., once a growing chain adds a bound monomer unit, it is more likely to add a neighboring bound B monomer than a random free A monomer. Overall, varying the concentration of free A monomers does not have an effect of the system behavior. This is due to the large excess of A monomers present in the system. In the following discussion, we thus set $[A] = 3125$ for most of the simulations.

We monitor the distribution of sequence lengths of A monomers in both the A homopolymer and A–B copolymer chains. Figure 4 shows a bimodal distribution of sequence lengths of A monomers for $[I] = 125$ and $[A] = 3125$ at different grafting densities of B on the substrate. At low grafting densities ($\sigma_B < 1$), the A unimers and dimers are much more abundant than longer A blocks. This is manifested by the maximum in the sequence length distribution (cf. Figure 4) of the A units. This distribution includes contributions from both A homopolymers and A–B copolymers. To better comprehend the distribution of A monomers in the two types of polymers, in the insets we plot separately the distribution of A sequences in A homopolymers (green) and A–B copolymers (red). As expected the A homopolymer sequence distribution is Gaussian in nature, with the mean corresponding to the average molecular weight of the homopolymers, irrespective of the grafting density of the bound monomers. This suggests that the presence of bound B monomers does not influence the formation of A homopolymer chains; the only factors influencing the length of the A homopolymers are the initial number of initiators and free monomers present in the system (see Supporting Information). In contrast, the distributions of A sequences in the A–B copolymers are strongly influenced by

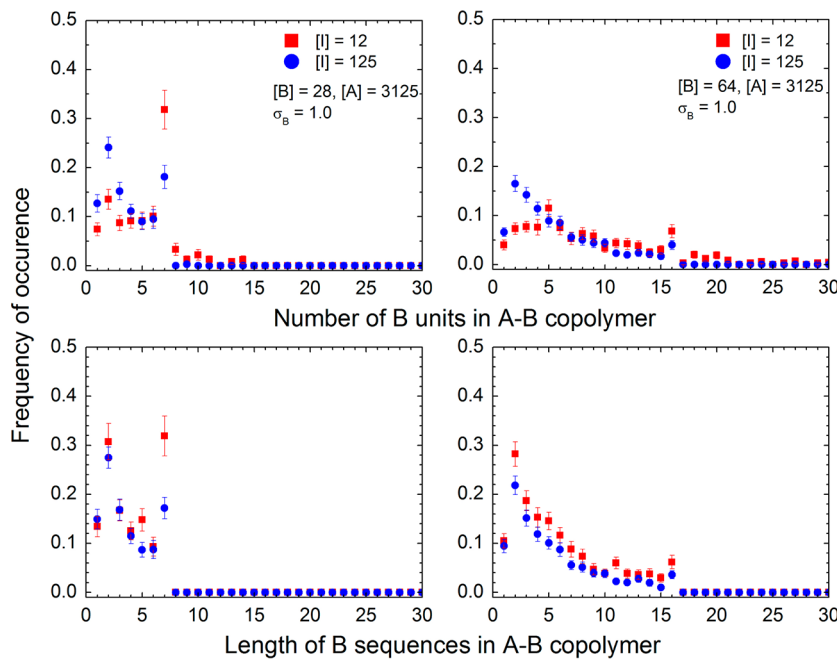


Figure 5. Effect of the number of initiators ($[I]$) and the number of bound B monomers ($[B]$) on the number distribution and sequence length distribution of B in copolymers A–B (averaged over 50 simulation runs).

the grafting density of B on the template. At low grafting density ($\sigma_B < 1$) the frequency of occurrence of short A runs is higher than that at $\sigma_B = 1$. These short sequence lengths of A act as linkers between the neighboring B units in the A–B copolymer. The number of linkers decreases when $\sigma_B = 1$.

The mean free A monomer sequence length is calculated to be approximately 10.3 ± 9.4 for low grafting densities ($\sigma_B < 1$) and 12.3 ± 6.8 for high grafting density ($\sigma_B = 1$). Our computer simulations indicate that for $\sigma_B < 1$ the B monomers are incorporated into the A–B copolymers as unimers; i.e., there are no dimers, trimers, tetramers, etc. constituting consequent runs of B units within the A–B chains. Only for $\sigma_B = 1$ we detect the presence of B-mers longer than unimers. This suggests that longer sequences of consecutive B runs can be realized when the B monomers are spaced on the substrate as closely as possible. We conclude that high grafting density promotes the polymerization of successive bound B monomers into a single chain and gives rise to random block copolymers with longer sequences of A and B, whereas at low grafting densities, it is more likely to form “truly random” copolymers with discretely and randomly distributed bound monomer (B) units.

This finding also reveals that varying the absolute value of $[B]$, while keeping $\sigma_B = 1$ should alter the population density of the various “mers”. In Figure 5, we compare the number and sequence length distributions of systems having different number of bound monomers ($[B] = 28$ and 64) at $\sigma_B = 1$. The sequence length distribution of B for $[I] = 12$ and $[B] = 28$ (left column, red squares) shows a distinct peak value corresponding to sequence length of 7, which corroborates the “proximity effect” (*vide supra*). Increasing $[I]$ 10-fold results in decreasing the average number of B units per A–B chain ten times, thus attenuating this “proximity effect”; we note that the distinct peak corresponding to sequence length of 7 found at $[I] = 12$ is greatly diminished while the overall distribution peaks at a sequence length of 2. The trends observed for $[I] = 12$, are replicated when $[I] = 64$ (corresponding to 16 B

monomers bounds on each substrate). For instance, the data in Figure 5 (right column) exhibit a distinct peak at sequence length of 16. The data also reveal that in the presence of a large number of bound B monomers the A–B copolymers are more likely to incorporate a greater number of B (>13) and possess longer sequences of B (>7). This behavior holds true regardless of the number of initiators present in the system. However, the frequencies of occurrence corresponding to number of B and sequence length equal to 16 (in case of $[B] = 64$; i.e., 16 B monomers per substrate) are much lower than the frequencies corresponding to 7 (in case of $[B] = 28$; i.e., 7 B monomers per substrate). This implies that for a greater number of bound B monomers on each substrate, it is less likely to incorporate all the B monomers in a single chain. Thus, the template length poses a practical limitation on the replication process leading to complementary polymer chains. Figure 6 shows a typical snapshot from one of the simulation runs, depicting the distribution of B monomers in A–B copolymers for $[I] = 125$, $[B] = 64$, and $[A] = 6250$. Each B monomer and A–B copolymer is assigned a serial number (shown along x and y axes in Figure 6, respectively). Monomers ranked 1–16, 17–32, 33–48, and 49–64 are attached to rod substrates ranked 1, 2, 3 and 4, respectively; the red lines demarcate the position of the substrates in Figure 6. We count the number of blocks of B segments in each copolymer, the corresponding block length (number of B in a block) and the serial number of each B monomer unit in a block and plot this information in Figure 5 for a visual representation. For example, consider polymer 1 in Figure 6. It has two B blocks of lengths 1 and 2 shown in black and yellow, respectively. The data in Figure 6 also reveal that both these blocks (monomer numbers 49, 50–51) are located on the fourth rod substrate.

Previous studies on template polymerization^{26–29} assume that the “sticky” units are reversibly adsorbed on the flat templates. Therefore, a copolymer chain is only partially adsorbed to the substrate at certain sites where there are blocks of “sticky” units. In contrast, we employ one-dimensional

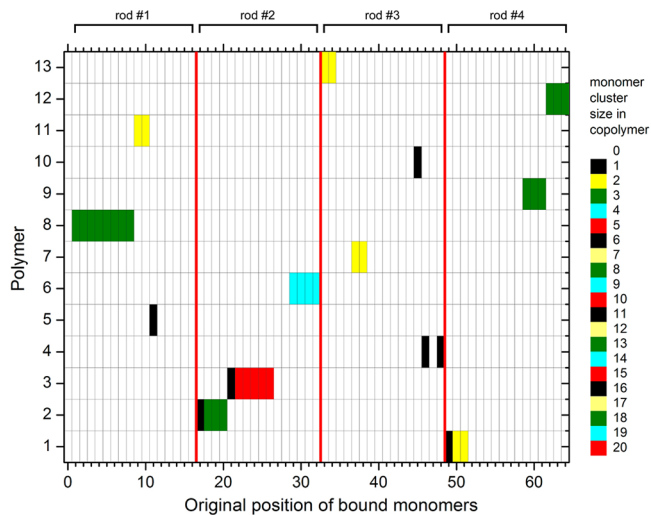


Figure 6. Distributions of “mers” in A–B copolymers for $[I] = 125$, $[B] = 64$, and $[A] = 6250$. Unimers to octamers are observed to be formed under these conditions (the red lines separate the monomers attached to different substrates).

substrates which do not restrict the mobility of the growing copolymer chain as much as a planar substrate. Once a growing chain incorporates a bound B monomer unit, it goes along the rod-like template to incorporate more B units (at $\sigma_B = 1$) or loops around as it incorporates the free A monomers. In this work we fix the number of B monomers initially and therefore impose physical limitations on the B-blocks by incorporating finite number of B on each template. Hence, a direct comparison of our results with those in previous studies²⁸ is not straightforward.

In the results discussed thus far, we kept the position as well as the orientation of the B monomers constant. To make the system more realistic, one has to consider that the orientation

of the B monomers on the substrate may change with time (while their position is fixed). This would correspond to situations, in which the B monomers are attached to the substrate via flexible linkers that allows the B units to alter their spatial orientation with time. Hence, next we explore the effect of flexibility of bound B monomers on their number distribution and sequence length distribution in the A–B copolymers. Figure 7 shows a comparison of the fixed (red squares) and flexible (blue circles) bound monomer cases for two systems ($[B] = 28$ or 64) at the maximum grafting density ($\sigma_B = 1$). The flexibility of B monomers dilutes the “proximity effect”; the average spacing between adjacent bound and flexible monomers does not remain constant through the run time, effectively reducing the overall grafting density. This is evident from the disappearance of peaks (red squares) corresponding to 7 (for $[B] = 28$) or 16 ($[B] = 64$) in the number distributions of B and the occurrence of discrete B units in sequence length distributions. Therefore, in systems featuring flexible bound B monomers one cannot polymerize all B monomers present on the substrate. Thus, the B monomers bound rigidly to the substrate (i.e., no conformational flexibility) are more favorable toward templation at high grafting densities.

Figure 8 shows a comparison of the number of A homopolymers and A–B copolymers as well as the composition of A–B copolymers formed with two different numbers of initiators, i.e., $[I] = 12$ (close symbols) and 125 (open symbols), at different σ_B for fixed (left column) and flexible (right column) bound B monomers. The red and blue symbols represent the data pertaining to A–B copolymers and A homopolymers, respectively. The number of A–B copolymers produced in the system is governed by the number of initiators and the number of bound B monomers. The data in Figure 8 reveal that when the bound B monomers are present in excess of the initiators (i.e., $[B] = 28$ and $[I] = 12$), the number of A–B copolymers formed is limited by the number of

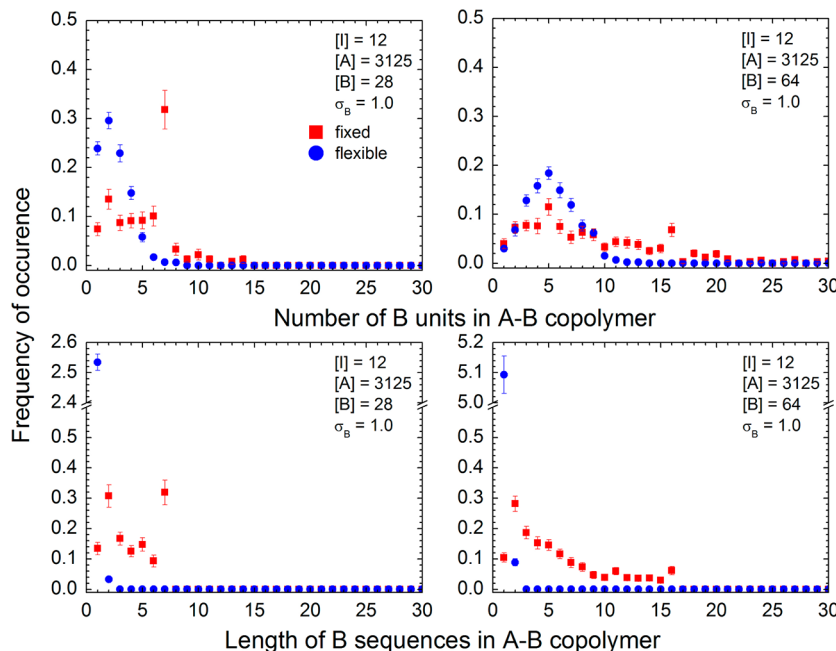


Figure 7. Effect of flexibility of the bound B monomers on the number distribution and sequence length distribution of B in A–B copolymers, averaged over 10 simulation runs, for $[I] = 12$ and $[A] = 3125$.

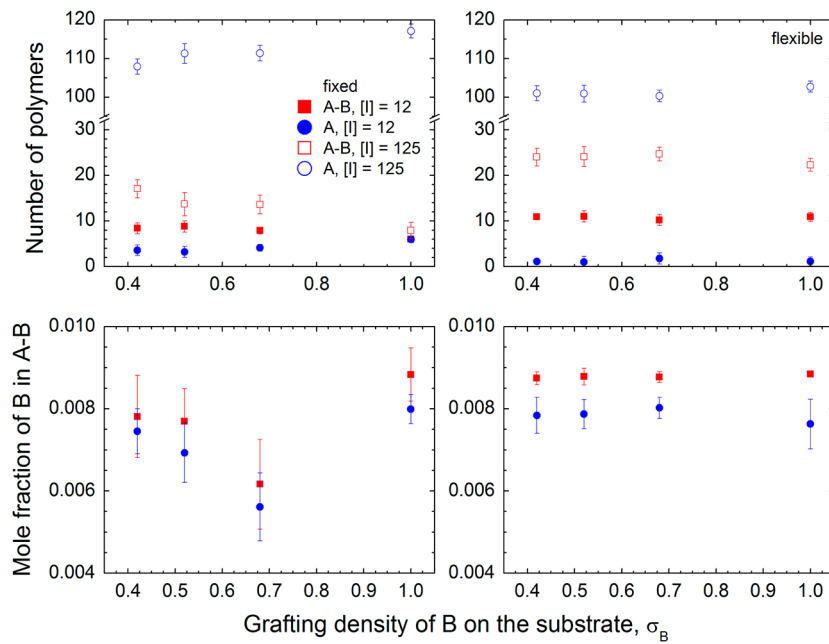


Figure 8. Average number of A polymers and A–B copolymers as well as the average A–B composition as a function of the grafting density of the B monomers (σ_B) in fixed (left column) and flexible (right column) conformations.

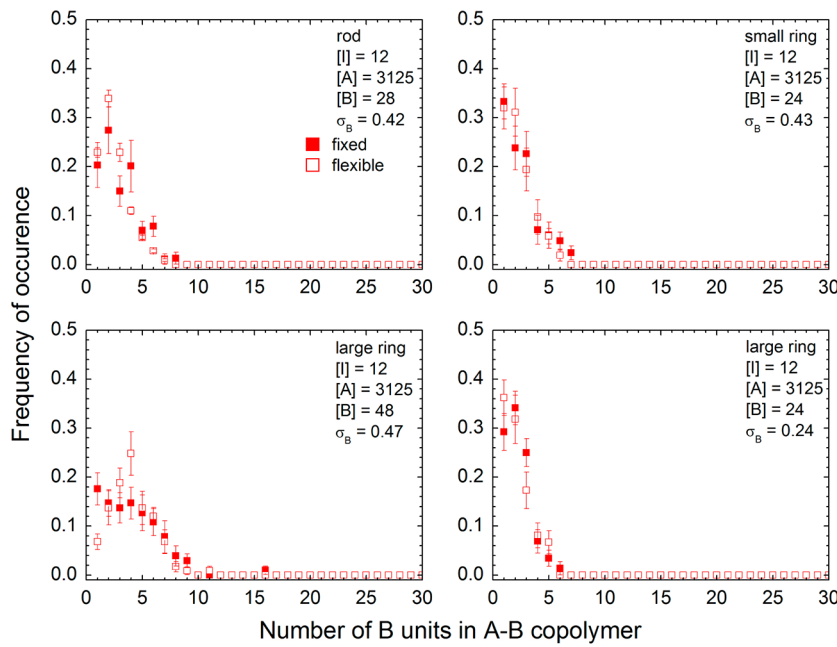


Figure 9. Comparison of the number distribution of B monomers in A–B copolymers for rod and ring-like substrates.

the initiators. In contrast, when the initiators are in excess ($[I] = 125$), the number of A–B copolymers formed is limited by the number of bound monomers ($[B] = 28$). This holds true at all grafting densities regardless of the flexibility of the B bound monomers. The fraction of B units in the A–B copolymers is slightly less in case of 125 initiators as compared to 12 initiators. Here, the greater the number of initiators results in more copolymers formed (*vide supra*); thus, the composition of the copolymers is limited by the number of bound B monomers present in the system. This argument is corroborated by a similar trend in the case of fixed bound B monomers. In addition, we observe that the mole fraction of fixed B in the A–B copolymers exhibits a minimum value at $\sigma_B = 0.68$

independent of $[I]$. Since the corresponding number of A–B copolymers does not show a maximum at $\sigma_B = 0.68$, we attribute the lower mole fraction of B to a lower overall number of B in the copolymers. High grafting densities can lead to steric hindrance of the growing chains, thereby attenuating the “proximity effect” that favors addition of bound B monomers. Since the steric effects increase with increasing σ_B the “proximity effect” predominates. The mole fraction data in Figure 8 for systems with fixed B monomers (right column) validate our hypothesis; the fraction of B in the A–B copolymers decreases with varying σ_B until $\sigma_B = 0.68$, and peaks at $\sigma_B = 1$. For flexible B bound monomers, both the number of polymers and the composition do not change

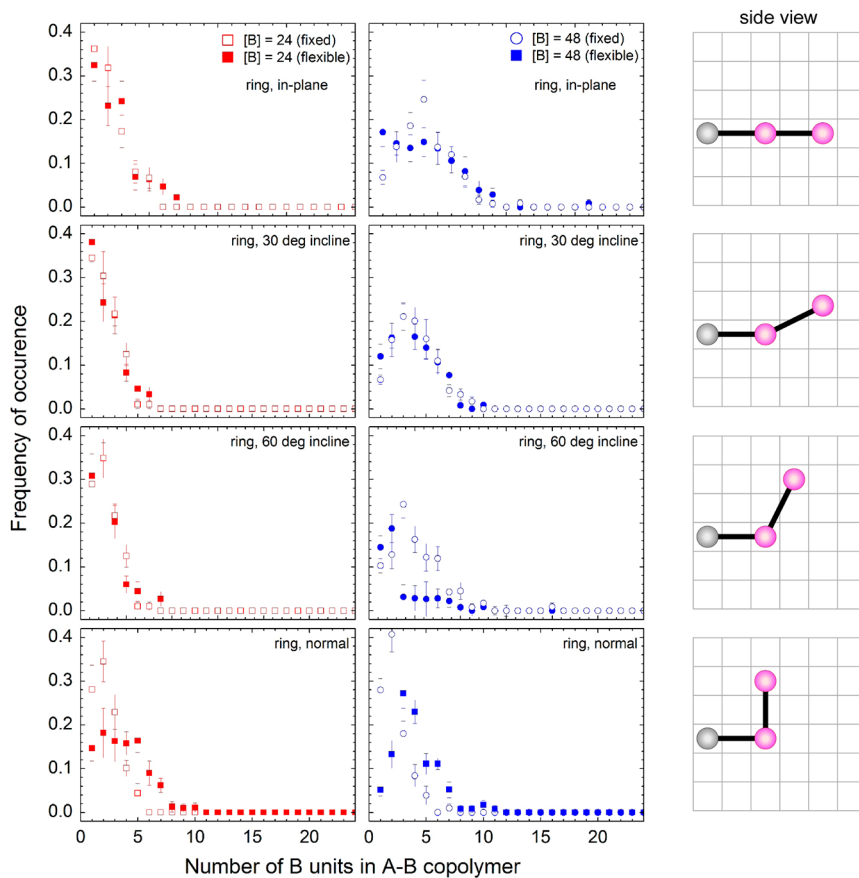


Figure 10. Effect of the orientation of the bound B monomer on their number distribution in A–B copolymers, averaged over 10 simulation runs, for $[I] = 12$, $[A] = 3125$ and $\sigma_B = 0.47$ (blue), 0.43 (red). The monomer orientation is shown pictorially in the right column.

significantly with increasing σ_B , most likely due to dilution of the “proximity effect” mentioned earlier.

In all simulation runs that have been discussed so far, we monitored the incorporation of bound B monomers (on rod-like substrates) into growing copolymer chains over time (not shown). We observed that regardless of its location on the rod-like substrate, each bound monomer on an average was equally likely to get incorporated in a copolymer chain and there is no preferred order of chain-growth along the template (i.e., there were no end-effects of the linear substrates). Intuitively, this is expected because the template is one-dimensional, which means that the B monomers located far away from the ends of the templates are as accessible to growing chains as the ones located at the two ends.

Thus, far, we have investigated cases, in which the B monomers were placed on 4 rigid rods placed uniformly in the lattice. In order to explore whether the geometry of the substrate plays a role in incorporating the bound B monomers into the A–B copolymers, we probe the effect of substrate shape and spatial orientation of the B bound monomers on the number distribution and the sequence length distribution of B in A–B copolymers. Figure 9 shows a comparison of rod and ring substrates with the same molecular parameters (i.e., $[I] = 12$, $[A] = 3125$ and $\sigma_B = 0.425 \pm 0.005$; top row). The number distributions show the same general trend for rod- and ring-shaped substrates, independent of chain flexibility. One striking observation is that both the systems (i.e., rod and ring) show the same maximum number of B units per A–B copolymer. However, the maximum number of B units per copolymer is

reduced when σ_B is decreased from 0.43 to 0.24. Similar to the rod-like substrates, the number distribution of B is affected by variations in σ_B ; at higher values of σ_B it is more likely to incorporate more bound B monomers in an A–B single chain. The data in Figure 9 also reveal that greater number of bound B monomers (i.e., $[B] = 48$) leads to an overall increase in incorporation of bound monomers per A–B copolymer and an increase in the maximum number of B per A–B copolymer. Thus, the substrate shape does not appear to affect the template polymerization process.

We have shown that the spatial orientation of the B monomers bound on the substrate affects the properties of the resultant A–B copolymers. In order to gain more insight into the effect of the spatial orientation of the B monomers relative to the orientation of the substrate, we placed the B monomers in various (fixed) positions along the ring-like substrate. Figure 10 shows the number distribution of B per A–B copolymer for four different spatial orientations of a bound monomer relative to the ring-like substrate (depicted pictorially by the cartoons on the right in Figure 10). The maximum number of bound B monomers that can be incorporated in a single A–B chain is dictated by the orientation of a bound B monomer relative to the ring-like substrate. Each orientation is marked by a characteristic peak in the number distribution of bound B monomers in the A–B copolymer. This peak shifts to the right as the orientation of the B monomers changes from in-plane to normal to the substrate. In ring-like substrates, the different spatial orientation of bound monomers effectively changes the spacing between adjacent bound monomers; the normal

orientation is the most densely packed while the in-plane one is the least packed. All parameters being the same, the difference in effective bound monomer spacing is most likely the reason behind the shift in the peaks in the number of B monomers in the A–B copolymer. For flexible B bound monomers, a similar trend is observed (not shown). The data also reveal that the maximum number of bound monomers incorporated per A–B copolymer increases slightly as the number of bound monomers is doubled. This is similar to the trend observed in case of rod-like substrates.

CONCLUSIONS

We used Monte Carlo simulations to investigate the effect of various factors, i.e., the grafting density (σ_B) and number of B bound monomers ([B]), the number of initiators ([I]), the number of free A monomers ([A]), and the flexibility of the bound monomers, on template polymerization involving rigid rod-like and ring-like substrates. The computer simulations ensured “true living” conditions by neglecting any chain termination or chain transfer. We noted that [A] has no significant influence on the template polymerization process as long as free A monomers are in excess; we thus chose to keep the number of free monomers constant ([A] = 3125) for most of the simulations present in this work. We observed that increasing σ_B increases the possibility of the bound B monomers to get incorporated into the growing A–B chains. At the maximum possible grafting density ($\sigma_B = 1.0$), the maximum number of B monomers gets incorporated into a single polymer chain. In addition, the maximum sequence length of “polymerized” bound B monomers increases with increasing the number of B monomers present on a single substrate; this effect is more significant when the bound B monomers lack any flexibility. At low σ_B , it is unlikely to form sequences of B longer than unimers. This behavior has been attributed to the “proximity effect” of the bound B monomers that favors the sequential polymerization of the bound monomers into a single growing chain. The effect of the grafting density is also manifested in the sequence length distribution of free A monomers in the copolymer chains; low grafting densities lead to “truly random” copolymers with mostly short A sequences intercepted by discrete B units while high grafting density favors the formation of random blocks of A and B in a copolymer chain. We also observed that increasing the number of initiators by 10-fold (12 to 125) leads to shorter sequence lengths of bound monomers and lowers the number of bound monomers present per polymer chain. Our computer simulations show that long sequences of B bound monomers are formed mostly when the bound B monomers are immobilized in space. We attribute this behavior to the dilution of the “proximity effect” in case of flexible bound B monomers as the average spacing between the adjacent B bound monomers does not remain constant throughout the simulation run. The number of A–B copolymers produced in the system is governed by [I] and [B] in the system. We showed that when the initiators are in excess (i.e., [I] = 125), the number of A–B copolymers formed is limited by the number of bound monomers (i.e., [B] = 28). Additionally, the chemical composition of the A–B copolymers is not significantly affected by increasing [I]. We also investigated the effect of substrate shape and orientation on template polymerization processes. All parameters remaining the same, the distribution of number of the bound B monomers incorporated per growing chain shows the same trend, irrespective of the shape of the

substrate (rod or ring) and the flexibility of the bound monomers, therefore there are no end effects associated with the rod-substrate. We also show that the maximum number of bound B monomers that can be incorporated in a single A–B chain is dictated by the spatial orientation of a bound monomer relative to the ring-like substrate. Each orientation is marked by a characteristic peak in the number distribution of bound B monomers. This peak shifts as the orientation of the B monomers changes from in-plane to normal to the substrate. We attribute this behavior to the change in the effective spacing between adjacent bound B monomers occurring due to different spatial orientations of the B monomers. The maximum number of bound B monomers incorporated per A–B copolymer increases slightly as [B] is doubled. This is similar to the trend observed in case of rod-like substrates.

Experimentally, the rod-like substrates can be realized in the form of functionalized nanowires or macro-molecules having monomeric units attached to a rigid backbone. Our simulations do not account for any flexibility or mobility of the substrates. It would be interesting to investigate whether substrate mobility promotes template polymerization. In the present work, we assumed that the bound and free monomers have identical reactivities. It would also be useful to carry out computer simulations to explore the effect of different reactivity ratios on the incorporation of bound monomers into growing polymer chains.

ASSOCIATED CONTENT

Supporting Information

Comparison of sequence length distributions. This material is available free of charge via the Internet at <http://pubs.acs.org>.

AUTHOR INFORMATION

Corresponding Author

*E-mail: jan_genzer@ncsu.edu.

Notes

The authors declare no competing financial interest.

ACKNOWLEDGMENTS

We thank the National Science Foundation for supporting this work through the grants No. CBET-0853667 and DMR-1121107 (Triangle MRSEC).

REFERENCES

- (1) Polowinski, S. *Template Polymerization*; ChemTec Publishing: Toronto, Canada, 1997.
- (2) Challa, G.; Tan, Y. Y. Template Polymerization. *Pure Appl. Chem.* **1981**, *53*, 647–651.
- (3) Rosenbaum, D. M.; Liu, D. R. Efficient and Sequence-Specific DNA-Templated Polymerization of Peptide Nucleic Acid Aldehydes. *J. Am. Chem. Soc.* **2003**, *125* (46), 13924–13925.
- (4) Gons, J.; Vorenkamp, E. J.; Challa, G. Radical polymerization of methyl methacrylate in the presence of stereoregular poly(methyl methacrylate). V. Kinetics of initial template polymerization. *J. Polym. Sci.: Polym. Chem.* **1975**, *13* (7), 1699–1709.
- (5) Smid, J.; Tan, Y. Y.; Challa, G. Effects of poly(2-vinylpyridine) as a template on the radical polymerization of methacrylic acid. I. Influence of atactic poly(2-vinylpyridine) concentration. *Eur. Polym. J.* **1983**, *19* (10–11), 853–858.
- (6) Rainaldi, I.; Cristallini, C.; Ciardelli, G.; Giusti, P. Kinetics and reaction mechanism of template polymerization investigated by conductimetric measurements. Part 3. Radical polymerization of acrylic acid in the presence of poly(*N*-vinylpyrrolidone). *Polym. Int.* **2000**, *49* (1), 63–73.

- (7) Shea, K. J.; Sasaki, D. Y. On the control of microenvironment shape of functionalized network polymers prepared by template polymerization. *J. Am. Chem. Soc.* **1989**, *111* (9), 3442–3444.
- (8) Serizawa, T.; Hamada, K.; Akashi, M. Polymerization within a molecular-scale stereoregular template. *Nature* **2004**, *429*, 52–55.
- (9) Hamada, K.; Serizawa, T.; Akashi, M. Template Polymerization Using Artificial Double Strands. *Macromolecules* **2005**, *38* (16), 6759–6761.
- (10) Trubetskoy, V. S.; Budker, V. G.; Hanson, L. J.; Slattum, P. M.; Wolff, J. A.; Hagstrom, J. E. Self-assembly of DNA-polymer complexes using template polymerization. *Nucleic Acids Res.* **1998**, *26* (18), 4178–4185.
- (11) Matsui, J.; Kato, T.; Takeuchi, T.; Suzuki, M.; Yokoyama, K.; Tamiya, E.; Karube, I. Molecular recognition in continuous polymer rods prepared by a molecular imprinting technique. *Anal. Chem.* **1993**, *65* (17), 2223–2224.
- (12) Wang, W.; Gao, S.; Wang, B. Building Fluorescent Sensors by Template Polymerization: The Preparation of a Fluorescent Sensor for d-Fructose. *Org. Lett.* **1999**, *1* (8), 1209–1212.
- (13) Ford, J. F.; Vickers, T. J.; Mann, C. K.; Schlenoff, J. B. Polymerization of a Styrene-bound Monolayer. *Langmuir* **1996**, *12* (8), 1944–1946.
- (14) Schweitz, L.; Anderson, L. I.; Nilsson, S. Capillary Electrophoresis with Predetermined Selectivity Obtained through Molecular Imprinting. *Anal. Chem.* **1997**, *69* (6), 1179–1183.
- (15) Schweitz, L.; Anderson, L. I.; Nilsson, S. Molecular imprinting for chiral separations and drug screening purposes using monolithic stationary phases in CEC. *Chromatographia* **1999**, *49*, S93–S94.
- (16) Lin, J. M.; Uchiyama, K.; Hobo, J. Enantiomeric resolution of dansyl amino acids by capillary electrochromatography based on molecular imprinting method. *Chromatographia* **1998**, *47*, 625–629.
- (17) Takuechi, T.; Haganaka, J. Separation and sensing based on molecular recognition using molecularly imprinted polymers. *J. Chromatogr. B: Biomed. Appl.* **1998**, *728* (1), 1–20.
- (18) Meier, W. Polymer Nanocapsules. *Chem. Soc. Rev.* **2000**, *29* (5), 295–304.
- (19) Meier, W.; Graff, A.; Diederich, A.; Winterhalter, M. Stabilization of planar lipid membranes: A stratified layer approach. *Phys. Chem. Chem. Phys.* **2000**, *2* (20), 4559–4562.
- (20) Graff, A.; Winterhalter, M.; Meier, W. Nanoreactors from Polymer-Stabilized Liposomes. *Langmuir* **2001**, *17* (3), 919–923.
- (21) Nardin, C.; Meier, W. Polymerizable Amphiphilic Block Copolymers: From Nanostructured Hydrogels to Nanoreactors and Ultrathin Films. *Chimia* **2001**, *55*, 142–146.
- (22) Bein, T.; Enzel, P. Encapsulation of Polypyrrole Chains in Zeolite Channels. *Angew. Chem.* **1989**, *28* (12), 1692–1694.
- (23) Carmesin, I.; Kremer, K. The bond fluctuation method: a new effective algorithm for the dynamics of polymers in all spatial dimensions. *Macromolecules* **1988**, *21* (9), 2819–2823.
- (24) Genzer, J. In silico polymerization: Computer simulation of controlled radical polymerization in bulk and on flat surfaces. *Macromolecules* **2006**, *39*, 7157–7169.
- (25) Turgman-Cohen, S.; Genzer, J. Computer Simulation of Controlled Radical Polymerization: Effect of Chain Confinement Due to Initiator Grafting Density and Solvent Quality in “Grafting From” Method. *Macromolecules* **2010**, *43* (22), 9567–9577.
- (26) Starovoitova, Y. N.; Berezkin, A. V.; Kriksin, Y. A.; Gallyamova, O. V.; Khalatur, P. G.; Khokhlov, A. R. Modeling of radical copolymerization near a selectively adsorbing surface: Design of gradient copolymers with long-range correlations. *Macromolecules* **2005**, *38* (7), 2419–2430.
- (27) Kuchanov, S. I.; Khokhlov, A. R. Theory of interphase free-radical copolymerization at the oil-water boundary. *Macromolecules* **2005**, *38* (7), 2937–2947.
- (28) Berezkin, A. V.; Khalatur, P. G.; Khokhlov, A. R. Simulation of gradient copolymers synthesis via conformation-dependent graft copolymerization near a uniform adsorbing surface. *Macromolecules* **2006**, *39* (25), 8808–8815.
- (29) Berezkin, A. V.; Solov'ev, M. A.; Khalatur, P. G.; Khokhlov, A. R. Template copolymerization near a patterned surface: Computer simulation. *J. Chem. Phys.* **2004**, *121* (12), 6011–6020.
- (30) Kennemur, J. G.; Novak, B. M. Advances in polycarbodiimide chemistry. *Polymer* **2011**, *52*, 1693–1710.